

Polymerization-Induced Phase Separation in Silica Sol-Gel Systems Containing Formamide

HIRONORI KAJI, KAZUKI NAKANISHI, AND NAOHIRO SOGA

Department of Industrial Chemistry, Faculty of Engineering, Kyoto University, Kyoto 606-01, Japan

Abstract. Silica gels with well-defined pores both in micrometer and nanometer ranges were obtained by acid-catalyzed hydrolysis and polymerization of tetramethoxysilane in the presence of formamide. The micrometer-range structures of these gels are studied in terms of the phase diagram of the quasi two-component system, namely solvent-rich and silica-rich end compositions. The resulting interconnected structures and aggregates of particles are related to the occurrence of spinodal phase separation. The composition region that gave interconnected structures for the present system was much more limited and their characteristic sizes were much smaller than those for the previously reported systems containing an organic polymer. These results could be explained qualitatively by the effect of the degree of polymerization on the Flory-Huggins' type free energy change of mixing.

Key words: Flory-Huggins' theory, phase separation, spinodal decomposition, sol-gel method, porous silica gel

1 Introduction

Structure formation during phase separation has been studied in various kinds of systems [1, 2], and intensive research into that of polymer mixtures has been carried out recently [3–10].

The mechanisms of phase separation can be classified into the spinodal decomposition (SD) type and nucleation-growth (NG) type. The NG occurs in the metastable region, while SD occurs in the unstable region; SD is often divided into initial, intermediate, and late stages.

The dynamics of liquid-liquid phase separation by isothermal demixing (temperature-jump method) of binary polymer blends (see Fig. 1a has been examined by Tanaka and Nishi et al. using digital-image-analysis (DIA) [3, 4] and real-time pulsed NMR [5]; and by Hashimoto et al. using light scattering (LS) [6, 7].

Inoue et al. have induced phase separation by curing reactions of liquid rubber-modified epoxy resins [8–10]. The mixture in a single-phase state at the early stage of curing is thrust into a two-phase region because the increase in the molecular weight of epoxy with the curing reactions elevates the binodal and spinodal lines (Fig. 1b). As against the "physical quench"

induced by a temperature-jump method, the method of inducing phase separation by a chemical reaction is often called "chemical quench."¹

We have already examined phase separations in silica sol-gel systems containing an organic polymer such as poly[sodium styrene-sulfonate] [12,13] or polyacrylic acid (HPAA) [14,15]. The hydrolysis and polymerization reactions of alkoxy silanes induced a phase separation between organic polymer-rich and silica-rich end compositions, in a manner similar to the curing systems of epoxy.

When alkoxy silanes react with water under the acid-catalyzed condition, they are immediately hydrolyzed to become polar. As these polar-hydrolyzed alkoxy silanes polymerize, the polar silanol sites are preferentially consumed by condensation reactions, and accordingly, the silica species gradually become less polar. Hence, phase separation similar to the systems containing an organic polymer was expected to occur by adopting highly polar solvents instead of organic polymers, because the solubility between polymerizing silica and polar solvents becomes lower as the polymerization reaction of hydrolyzed alkoxy silanes proceeds.

In this report, phase separation of a system

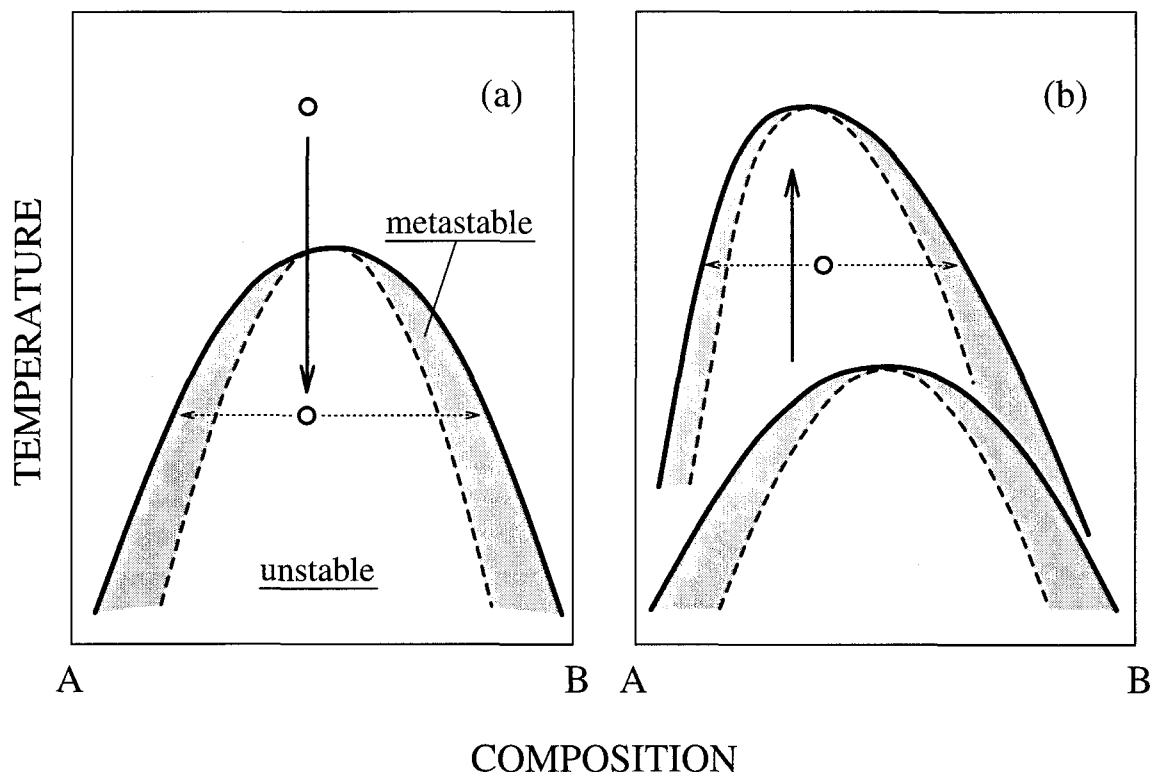


Fig. 1. Schematic phase diagrams of quasi two-component systems. Solid and broken curves are binodal and spinodal lines, respectively. Temperature-jump (a) or chemical reaction (b) brings the system, indicated by open circle, into two phase region. Processes (a) and (b) are called "physical quench" and "chemical quench," respectively.

in which alkoxy silanes are hydrolyzed and polymerized under the acid-catalyzed condition using formamide (FA) as a solvent was examined, and compared with that of the system containing HPAAs as an organic polymer [14,15].

2 Experimental

The sample gels were prepared as follows. FA was mixed with an appropriate concentration of aqueous solution of nitric acid. Tetramethoxysilane (TMOS) was added to this solution in a short time with stirring. Reactions were conducted at 0°C in order to prevent the evaporation of the constituents by the heat of reaction. The representative starting compositions

are listed in Table 1. The solution immediately became homogeneous, and after one minute's stirring, it was poured into two containers. Each container was sealed and was kept at 40°C or 60°C for gelation and aging for one day. The gelation time, t_g , was determined as the time when the sample lost its fluidity, and the phase separation time, t_{ps} , was determined as the time when the sample lost its transparency. Each of the wet gels thus obtained was divided into two pieces and immersed either in about fourfold volume of 1M nitric acid (1MNA) or methanol (MeOH) for one day, and finally dried at 60°C for two days.

A scanning electron microscope (SEM S-510) was employed for the observation of morphology using fractured surfaces of the dried gels obtained as above. The sizes of silica skeletons,

Table 1. Typical starting compositions for FA-system.

Sample	TMOS	FA	Aqueous solution of nitric acid		Molar ratio of TMOS:FA: water
H-1.6	10ml	7.620g	1.0M	2.079g	1:2.5:1.6
H-1.4	10ml	7.620g	1.0M	1.819g	1:2.5:1.4
N-0.6	10ml	7.620g	0.6M	1.899g	1:2.5:1.5
N-1.0	10ml	7.620g	1.0M	1.949g	1:2.5:1.5
N-1.4	10ml	7.620g	1.4M	2.000g	1:2.5:1.5
F-2.6	10ml	7.925g	1.0M	1.949g	1:2.6:1.5

spherical particles, and pores were evaluated by the direct measurements on the SEM photographs.

The pore size distributions above $10^{-2}\mu\text{m}$ of some dried gels were determined by Hg porosimetry (PORESIZER-9310). The measurements of pore size distributions below $10^{-1}\mu\text{m}$ were carried out by N_2 adsorption-desorption measurements (ASAP-2000) in which desorption data were used. In this method, the measurements for the as-dried gels could not be carried out, because they contained considerable amounts of solvents. Thermal analyses of the as-dried gels by TG-DTA system (TAS-100) indicated that the solvents were almost completely decomposed or evaporated by heat-treatment up to 300°C . Thus, the gels heated with the rate of $100^\circ\text{C}/\text{h}$ and held at 300°C for 2h were used instead of the as-dried ones. The preparation of the samples containing HPAA with average molecular weight of 90,000 (the degree of polymerization is ~ 1250) is described in our previous papers [14,15]. The representative starting compositions are listed in Table 2.

3 Results

The micrometer-range structures of resultant dried gels are classified into four typical morphologies as shown in Fig. 2. They are named a homogeneous gel, an interconnected structure, aggregates of particles, and a macroscopic two-phase, respectively. A 'homogeneous gel' appeared transparent or translucent and its pore sizes were under the range of several tens nanometers. In an 'interconnected structure,' both the silica skeleton and pores were cocon-

tinuous, and the characteristic size (defined as the length of the thickness of the silica skeleton plus the pore diameter) was from submicrometer to micrometer range. An interconnected structure with characteristic size above $10\mu\text{m}$ was not obtained in the present system. 'Aggregates of particles' also had the cocontinuous silica skeleton and pores, but the thickness of the silica skeleton was not uniform; instead, particles of a few micrometers were connected necks with each other. A 'macroscopic two-phase' was formed when liquid-liquid phase separation occurred and was followed by the gelation of the precipitated silica-rich phase gradually from the bottom. In the photograph of a macroscopic two-phase in Fig. 2, only the silica-rich phase is shown. Isolated pores contained in the condensed silica matrix are assumed to be the spaces filled with the solvent-rich phase in the wet state, which could not escape from the silica-rich phase before gelation.

The pore size distributions of representative gels, the morphologies of which were an interconnected structure and aggregates of particles, are shown in Fig. 3. The gel with an interconnected structure has dual porosity and the pores are quite uniformly distributed around $3\mu\text{m}$ and below 4nm . The gel composed of aggregates of particles also has dual porosity and the pores are rather widely distributed around $6\mu\text{m}$ and below 4nm . These gels had very high porosities, which reached 70–80% when the skeletal density is taken to be equal to $2\text{g}/\text{cm}^3$ [16].

In this report, we focus on the micrometer-range structures. The nanometer-range structures are discussed in detail elsewhere [17].

Figure 4 shows the effect of solvent exchange treatment for as-aged gels on the micrometer-

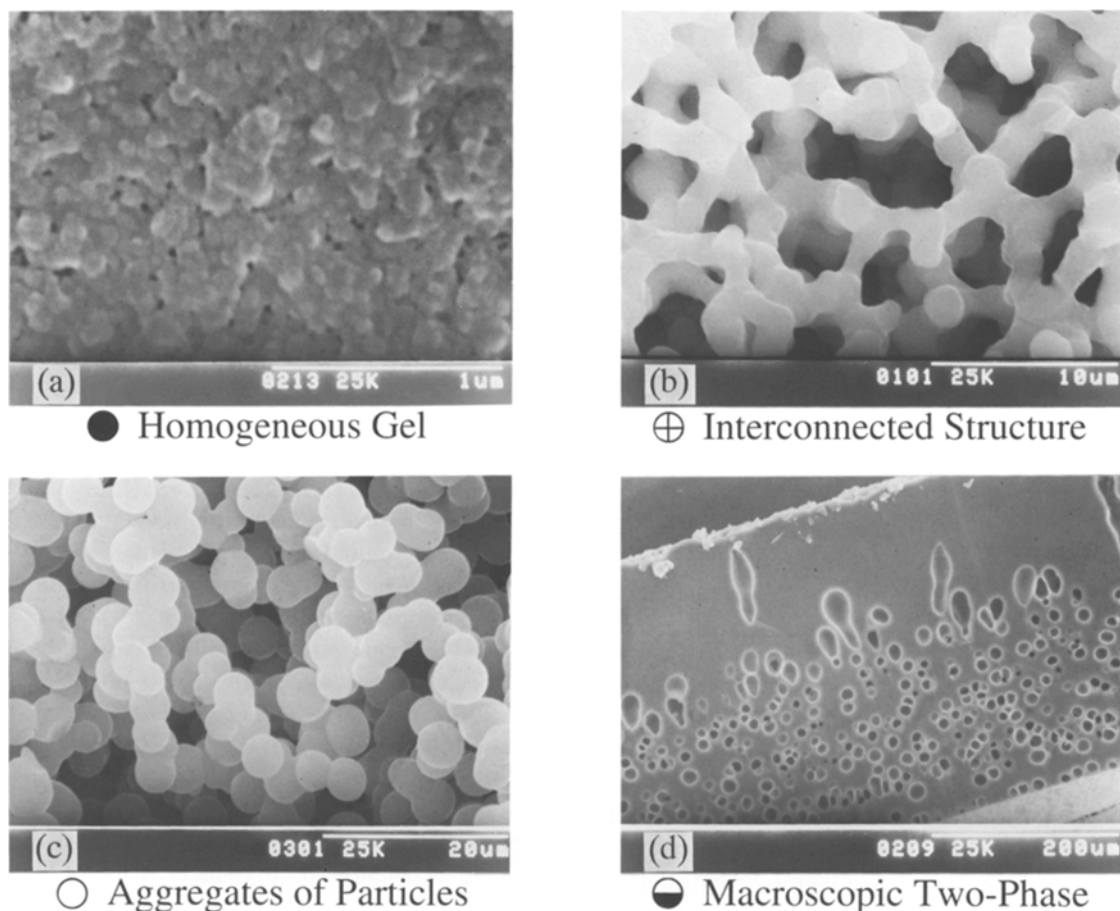


Fig. 2. SEM photographs of typical gel morphologies with respective symbols. Each gel is (a) H-1.6, (b) N-0.6, (c) N-1.4, and (d) H-1.4. All the gels are gelled and aged at 40°C, and soaked in 1MNA. Photograph of a macroscopic two-phase shows only a silica-rich phase.

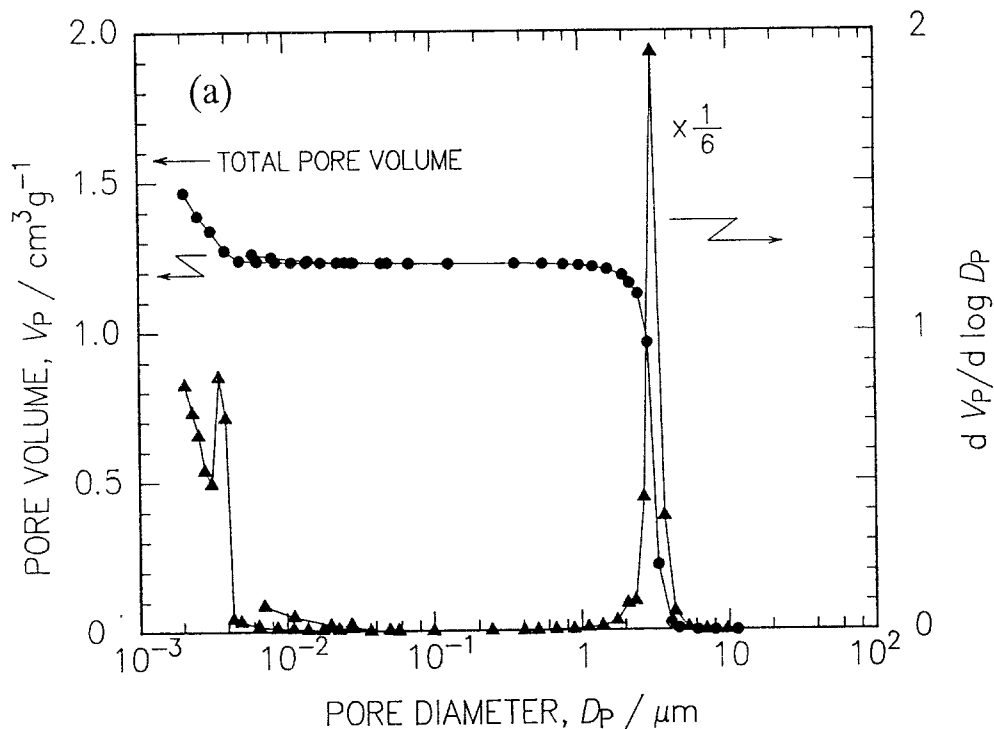
Table 2. Typical starting compositions for HPAA-system.

Sample	TEOS	EtOH	Aqueous solution of nitric acid		HPAA (M.W. 90,000)
HPAA1	7ml	3.0ml	1.0M	4.40g	0.40g
HPAA2	7ml	4.0ml	1.0M	3.30g	0.40g

range structure. When gels are soaked in 1MNA, additional reactions proceed, while soaking in MeOH arrests further reactions [17]. However, neither a change of morphology nor of the characteristic size of the micrometer-range structure was observed. Hg porosimetry measurements for dried gels exhibited the same result. Thus, we can confirm that micrometer-range structures are fixed during the gelation

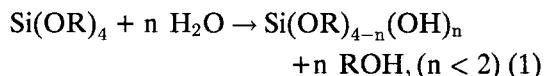
and one day's aging processes. All the other samples exhibited the same results.

Relations between compositions and morphologies of resultant gels are shown in Fig. 5 for the present system (a) and for the system containing HPAA (b). Hereafter, the present system (a) and the system containing HPAA (b) are respectively referred to as FA-system and HPAA-system. For both systems, the concen-



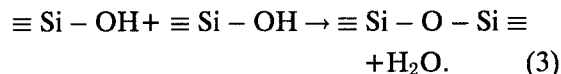
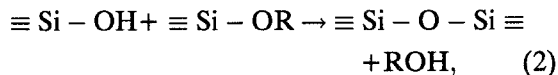
(continued)

tration of aqueous solution of nitric acid was fixed at 1M, and for HPAAsystem, the molar ratio of monomeric unit of HPAAs to Si was fixed at 0.177. The solution composition changes with the progress of reactions, and the morphologies of gels must be related not to the initial compositions but to the compositions at the time of phase separation. For FA-system, it was assumed that the initially added water was entirely consumed for the hydrolysis reaction (1),

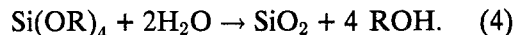


and the concentration of water became effectively zero by the time of phase separation, because less than 2 mol of water per 1 mol of alkoxy silane was used. Thus, the compositions at phase separation were calculated on the assumption that all the initially added water was consumed to produce the equivalent mol of alcohol from the starting composition. The real solvent composition may shift to the alcohol-rich side, because additional alcohol is generated both by the polymerization reaction (2) and by the hydrolysis reaction (1) using the water

regenerated by the polymerization reaction (3).



For HPAAsystem, it was assumed that alkoxy silane species were hydrolyzed and polymerized completely by the time of phase separation, because more than 4 mol of water was used [14,18]. This implies the consumption of 2 mol of water and the production of 4 mol of alcohol per 1 mol of alkoxy silane from the starting composition:



Thus, gels were obtained in the region where the molar ratio of EtOH/Si is larger than 4. The possible highest concentration of Si, EtOH/Si = 4, are indicated in Fig. 5b as a broken line. Each composition triangle was constituted by a polar solvent (FA or water) existing in excess, a cosolvent (MeOH or EtOH), and polymerized silica. It is obvious that the composition region that gave interconnected structures

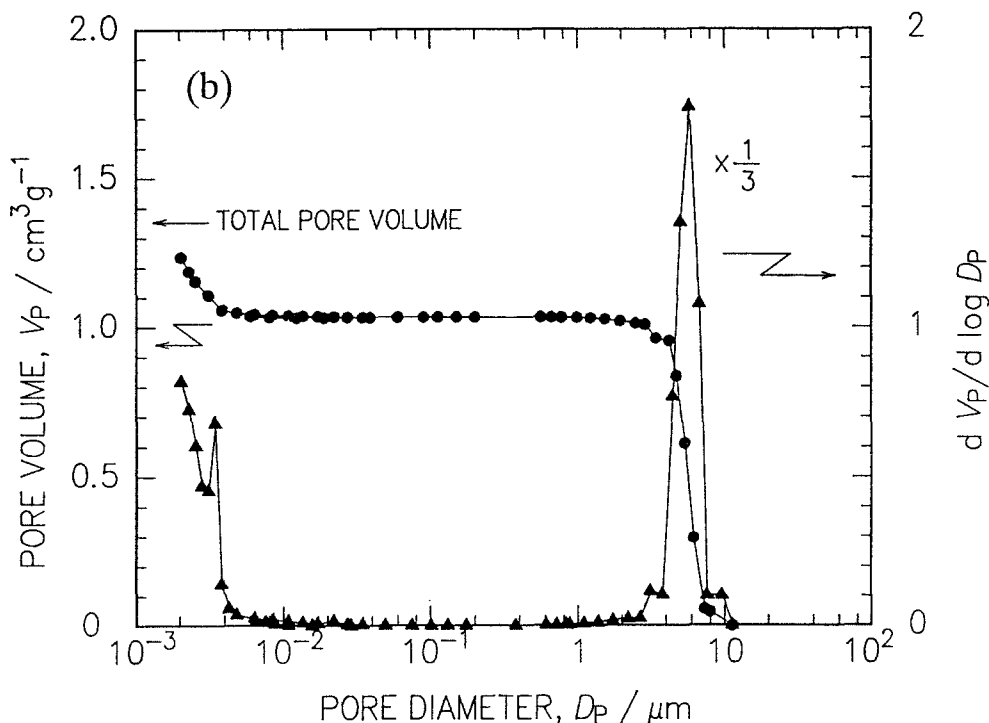


Fig. 3. Pore size distribution curves of gel samples gelled and aged at 40°C, and soaked in 1MNA. Their morphologies are (a) an interconnected structure (N-0.6), and (b) aggregates of particles (N-1.0). Closed circle denotes pore volume (V_p) and closed triangle denotes differential pore volume ($dV_p/d \log D_p$). The measurements above $10^{-2} \mu\text{m}$ are carried out by Hg porosimetry, and below $10^{-1} \mu\text{m}$, by N_2 adsorption-desorption method. Values of differential pore volumes measured by Hg porosimetry are divided by (a) six and (b) three.

Table 3. Porosities and characteristic sizes of typical gels for each system.

Sample	System	Pore* volume	Porosity*	Thickness of silica skeleton	Pore diameter	Characteristic size
N-0.6	FA	1.23cm ³ /g	71%	1.6μm	3.1μm	4.7μm
HPAA1	HPAA	0.34cm ³ /g	40%	6.0μm	4.2μm	10.2μm

*The values are only for the micrometer-range pores. The pore volumes and porosities for the nanometer-range pores are not included.

for FA-system is much more limited than that for HPAA-system.

The average micrometer-range characteristic sizes of gels whose morphologies are interconnected structures and aggregates of particles are included in Fig. 5. The sizes of aggregates of particles are generally larger than those of interconnected structures. The sizes of interconnected structures for FA-system are limited below 10 μm. This is in contrast with HPAA-system, where the sizes of interconnected structures is up to 100 μm.

The micrometer-range pore volumes of gels whose morphology was an interconnected structure were 1.2 – 1.4 cm³/g for FA-system, and 0.26 – 0.35 cm³/g for HPAA-system. The pore volume of a gel for FA-system is much larger than that for HPAA-system. The pore volumes, the porosities, the thicknesses of silica skeletons, the pore diameters, and the characteristic sizes of representative gels for each system are listed in Table 3. The SEM photographs of gels for HPAA-system are shown in Fig. 6. The silica skeletons of these gels are much thicker than

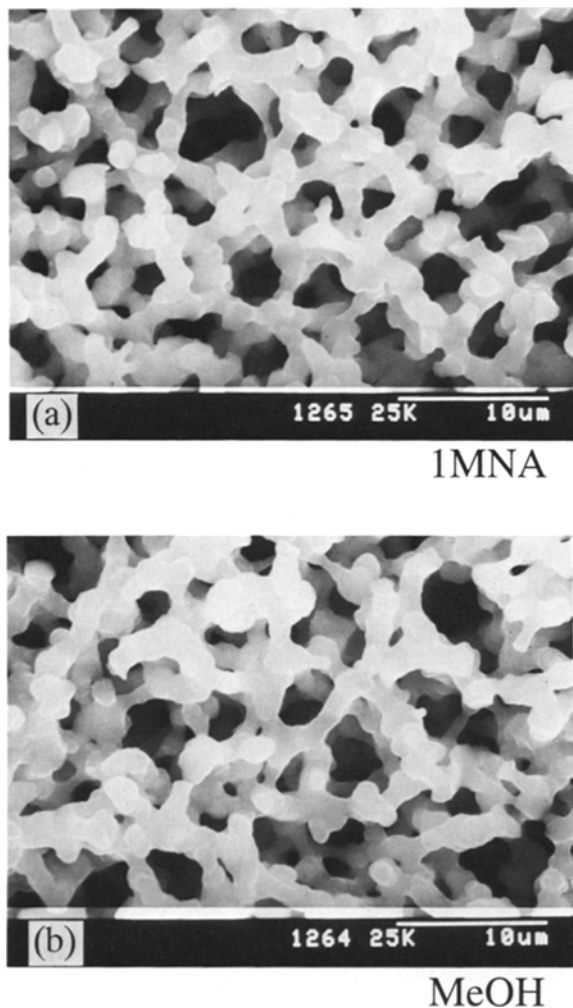


Fig. 4. Variation of the structures by solvent exchange treatment. These gels are F-2.6, gelled and aged at 60°C, and soaked in (a) 1MNA and (b) MeOH.

those for FA-system shown in Figs. 2b and 4. The same trend was observed for the other gels.

The effect of the molar ratio of FA to Si, f , on t_g , t_{ps} , and the resultant gel morphologies is shown in Fig. 7. The molar ratio of H₂O/Si was fixed at 1.5, which corresponded to the dotted line in Fig. 5a. Observed relations between the morphologies of dried gels and t_g , t_{ps} were as follows:

1. When $t_g \ll t_{ps}$, homogeneous gels were formed.
2. When $t_g \simeq t_{ps}$, interconnected structures were

formed. Aggregates of particles were formed when gelation occurred a little later.

3. When $t_g \gg t_{ps}$, macroscopic two-phases were formed.

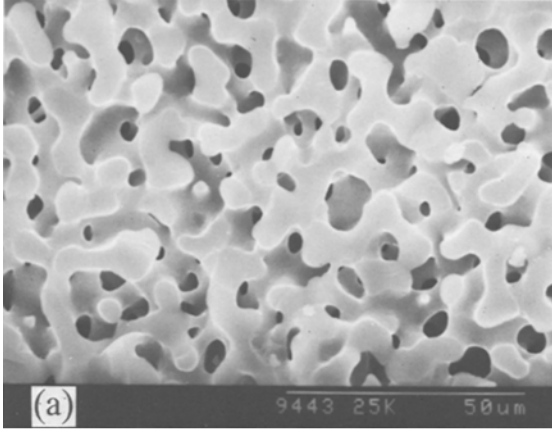
4 Discussion

4.1 Morphologies and Phase Separation Mechanism

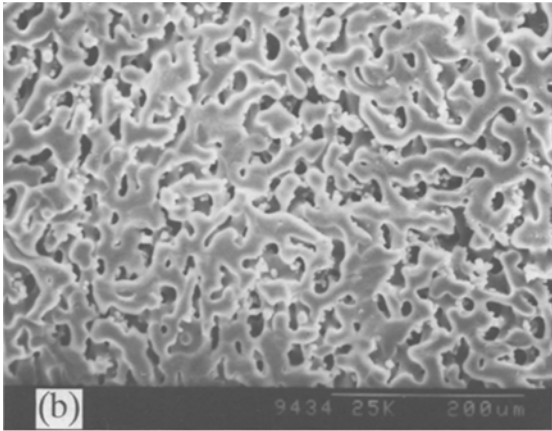
The present system can be assumed to have a phase diagram that consists of two components. In the systems containing an organic polymer [12–15], the formation of various gel morphologies was consistently explained in terms of the concurrent occurrence of phase separation and gel-formation induced by the polymerization of silica. The solution containing an organic polymer, alkoxy-derived silica, catalyst, and water could be regarded as a quasi two-component, silica-rich and organic polymer-rich, system. The present system, which contains FA, alkoxy-derived silica, catalyst, and water can be also regarded as a quasi two-component system. Phase separation will occur between polymerized silica and its solvent mixture, which results in the formation of silica-rich and solvent-rich phases.

Phase separation in these systems can be initiated by “chemical quench,” the rise of binodal and spinodal lines due to the polymerization of a component, which thrusts a single-phase mixture into a two-phase region. A transient structure that has been developed by phase separation is fixed as a permanent gel structure through gel-formation, and the structures of resultant dried gels reflect the transient structures in the various stages of the phase separation. Thus, a more developed state of phase separation is reflected in resultant gel morphologies obtained with the increased amount of FA, because longer time until gelation was available for the transient structure to grow (see Fig. 7).

From this consideration, the phase separation in this system is assumed to proceed through the following stages: (1) homogeneous solution,



HPAA1



HPAA2

Fig. 6. SEM photographs of gels of (a) HPAA1 and (b) HPAA2. These gels are gelled and aged at 40°C, and soaked in water-ethanol solution.

a narrow distribution, and the particles, held at the position of an interconnected silica skeleton, are almost uniform as observed in Fig. 2c. On the other hand, if phase separation occurred by NG mechanism, the discrete particles, generally called nuclei, would be formed at first to become aggregates of particles. To be developed into an interconnected structure, depolymerization and repolymerization of bonds in these particles, or attachment of siloxane oligomers in the solvent phase to the necks between particles, would be necessary. These processes are unlikely to occur

under acidic conditions where the solubility of silica is quite low [19,20], and are contradictory to the above experimental observations.

Thus, it is highly probable that the phase separation mechanism is not NG type but SD type. To confirm this hypothesis, the phase separation mechanism during the reactions must be examined by in situ methods such as LS or DIA.

4.2 Comparison with the System Containing an Organic Polymer

An addition of a small amount of an organic polymer makes it easy to obtain interconnected structures. The composition region that gave interconnected structures in FA-system was much smaller than that in HPAA-system, and FA-system could not give the interconnected structures above 10 μm of the characteristic size as against HPAA-system, which could give those around 100 μm . Interconnected structures with thick silica skeletons were obtained in HPAA-system, while interconnected structures obtained in FA-system had only thin silica skeletons, irrespective of the characteristic size range.

These differences can be explained in terms of the Flory-Huggins' theory [21]. This theory, based on the lattice model of polymeric mixture, gives the free energy change of mixing of a two-component system as

$$\Delta G = (N_T/\beta)\{(\phi_1/P_1)\ln\phi_1 + (\phi_2/P_2)\ln\phi_2 + \chi\phi_1\phi_2\}, \quad (5)$$

where ϕ_i and P_i are volume fraction and the degree of polymerization of component i ($i = 1$ or 2), respectively. $\beta = 1/k_B T$ is the inverse temperature, N_T is the total number of lattice cells in the system, and χ is the interaction parameter.² The critical point is given at the point that the binodal and spinodal lines coincide, where the following equation is satisfied:

$$(\partial^2 \Delta G / \partial \phi^2)_{T,P} = (\partial^3 \Delta G / \partial \phi^3)_{T,P} = 0. \quad (6)$$

From equations (5) and (6), the critical composition of component 2, ϕ_{2c} , is given by

$$\phi_{2c} = 1/\{1 + (P_2/P_1)^{1/2}\}. \quad (7)$$

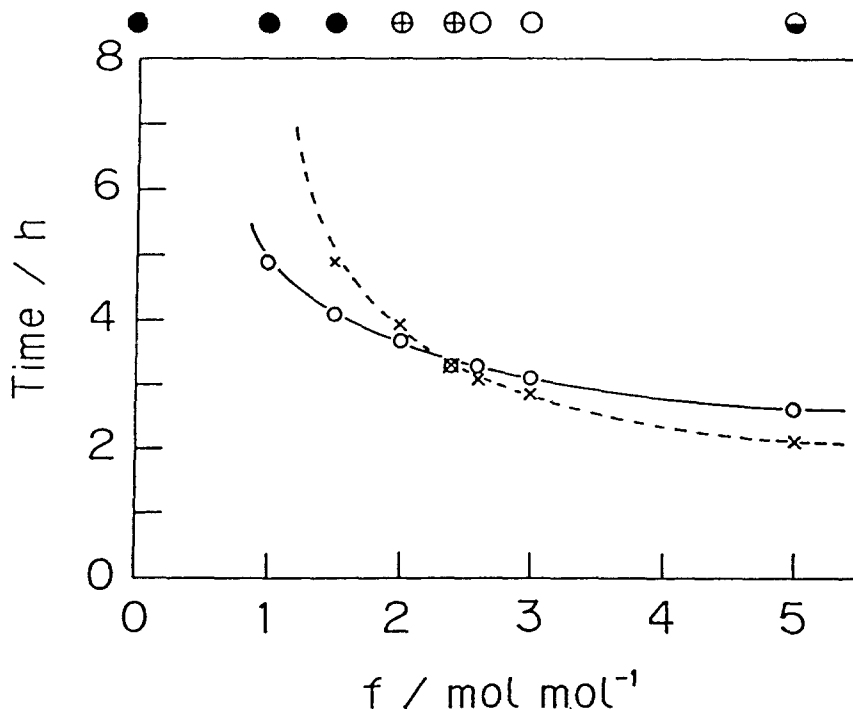


Fig. 7. Dependence of $t_g(o)$ and $t_{ps}(x)$ on the amount of FA under the condition of the molar ratio of $H_2O/Si = 1.5$. Above the figure, resultant gel morphologies are shown; ●, homogeneous gel; ⊕, interconnected structure; ○, aggregates of particles, ⊙, macroscopic two-phase.

When the above two systems are both considered as quasi two-component systems, components 1 and 2 correspond to solvent-rich or organic polymer-rich phase and silica-rich phase, respectively. Then, equation (5) with $P_1=1$ can be used in FA-system. While in HPA-system, the resultant organic polymer-rich phase contains solvents, thus the degree of polymerization of an organic polymer (~ 1250) cannot be used as it is. Nevertheless, P_1 for HPA-system would be much larger than unity. Interconnected structures and aggregates of particles were obtained when $t_g \simeq t_{ps}$ (Fig. 7), thus phase separation will not occur until the degree of polymerization of silica, P_2 , becomes quite large. Therefore, during phase separation, ϕ_{2c} for FA-system is much smaller, and binodal and spinodal lines are more asymmetric than those for HPA-system.³ This difference is schematically shown in Fig. 8. Here, we neglect the changes of the volume fraction and the interaction parameter on the assumption that the

change of the degree of polymerization of silica is much more effective than those two factors.

For the isothermal demixing, interconnected structures are more easily obtained in the composition region around the critical one. This is because, as the composition of the system approaches the critical one, SD-type phase separation occurs more easily and the continuities of interconnected domains of each phase, which emerge in the early stage of SD, are maintained without breakup during the following coarsening process [23,24]. Similarly, for the systems that induce phase separation by chemical quench, interconnected structures are also expected to be obtained more easily in the composition region around the critical one. Thus, the composition region in FA-system that gives interconnected structures would be more silica-poor than that in HPA-system (see Fig. 8). It results in the formation of continuous but thinner silica-rich phase. Besides, the viscosity of FA-system was much lower than that of

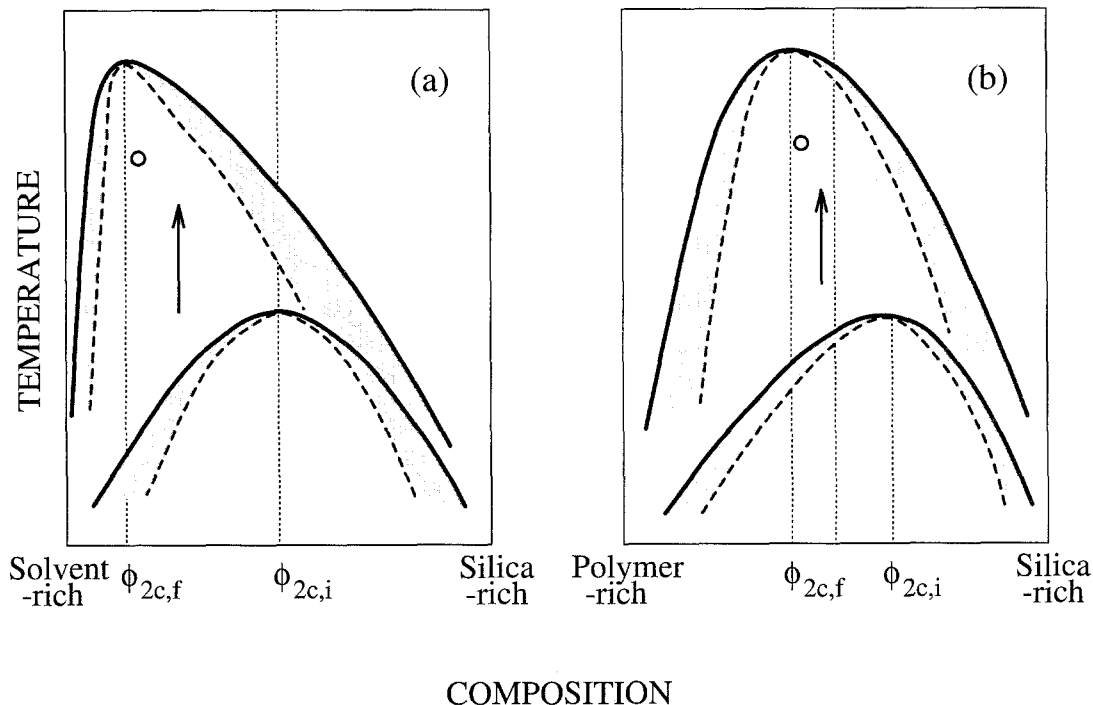


Fig. 8. Schematic phase diagrams for the present system containing FA (a), and the system containing an organic polymer (b). $\phi_{2c,i}$ and $\phi_{2c,f}$ are critical compositions just after all the constituents are mixed and during phase separation, respectively. $\phi_{2c,f}$ in FA system is much smaller, and binodal and spinodal lines are more asymmetric than those in HPAAsystem.

HPAA-system. The low volume fraction of the silica-rich phase and the low viscosity in FA-system induce the breakup and the following sedimentation of silica-rich domains during the earlier stage of a phase separation. Thus, interconnected structures easily become aggregates of particles or macroscopic two-phases during the coarsening process.

At least partly for these reasons, the present system cannot give interconnected structures whose characteristic size is as long as that of the system containing an organic polymer, and the composition region that gives interconnected structures is very restricted. In order to obtain interconnected structures with longer characteristic sizes or in broader composition region, it may be necessary to use the viscous system, which consists of end members with similar degrees of polymerization.

5 Conclusions

Interconnected structures could be obtained in a system containing TMOS, formamide, nitric acid, and water. The composition region that gave the interconnected structures for this system was much smaller than that for the system containing an organic polymer, and the former system could not give the interconnected structures with the characteristic sizes above $10 \mu\text{m}$. These results were well explained by regarding the above two systems as quasi two-component systems and assuming the phase diagram based on the Flory-Huggins' theory. The phase separation mechanism is presumably a spinodal decomposition type. To corroborate this mechanism, supplementary information about the phase separation during the reactions is now being collected.

Acknowledgments

The authors wish to acknowledge the contribution of Mr. Kawaguchi and Ms. Yamamoto, Advanced Glass R&D Centre, Asahi Glass Company Ltd. for carrying out Hg porosimetry measurements. Financial support from a Grant-in-Aid for Scientific Research, Priority Areas, New Functionality Materials, Design, Preparation and Control from the Ministry of Education, Science and Culture, Japan, is gratefully acknowledged.

Notes

1. In Figs. 1 and 8, the phase diagram of the present system is expressed as upper critical solution temperature (UCST) type, but the phase diagram is not defined up to now as to whether it is UCST type, lower critical solution temperature (LCST) type, or UCST-LCST coexisting type. Even if it is not UCST type, however, the compatibility of the system decreases with the increase of molecular weight [11], thus the mixture is thrust into a two-phase region with the progress of polymerization reactions.
2. Here, the χ parameter includes all the other factors affecting the free energy change of mixing except for the combinatorial entropy, e.g., the volume change of mixing of each constituent, their dipole interaction, as well as their van der Waals interaction.
3. The pore volumes of the system containing poly ethylene oxide (PEO) as an organic polymer are close to those of FA-system [22]. This seems to be contradictory to the discussion here, but in this case, the system phase-separates into one phase rich in PEO and silica, and the other rich in solvent.

References

1. J.D. Gunton, M. San Miguel, and P. Sahni in *Phase Transition and Critical Phenomena*, edited by C. Domb and J.H. Lebowitz (Academic, London, 1983), vol 8.
2. S. Komura and H. Furukawa, eds., *Dynamics of Ordering Processes in Condensed Matter* (Plenum, New York, 1987).
3. H. Tanaka and T. Nishi, *Phys. Rev. Lett.* **59**, 692 (1987).
4. H. Tanaka, *Phys. Rev. Lett.* **65**, 3136 (1990).
5. H. Tanaka and T. Nishi, *J. Appl. Phys.* **60**, 1306 (1986).
6. T. Izumitani and T. Hashimoto, *J. Chem. Phys.* **83**, 3694 (1985).
7. T. Izumitani, M. Takenaka, and T. Hashimoto, *J. Chem. Phys.* **92**, 3213 (1990).
8. K. Yamanaka and T. Inoue, *Polymer* **30**, 662 (1989).
9. K. Yamanaka, Y. Takagi, and T. Inoue, *Polymer* **30**, 1839 (1989).
10. K. Yamanaka and T. Inoue, *J. Mater. Sci.* **25**, 241 (1990).
11. For example, T. Nishi and TK. Kwei, *Polymer*, **16**, 285 (1975) for LCST system and S. Saeki, N. Kuwahara, S. Konno, and M. Kaneko, *Macromolecules*, **6**, 589 (1973) for UCST-LCST coexisting system.
12. K. Nakanishi and N. Soga, *J. Am. Ceram. Soc.* **74**, 2518 (1991).
13. K. Nakanishi, N. Soga, H. Matsuoka, and N. Ise, *J. Am. Ceram. Soc.* **75**, 971 (1992).
14. K. Nakanishi and N. Soga, *J. Non-Cryst. Solids* **139**, 1 (1992).
15. K. Nakanishi and N. Soga, *J. Non-Cryst. Solids* **139**, 14 (1992).
16. C.J. Brinker, G.W. Scherer, and E.P. Roth, *J. Non-Cryst. Solids* **72**, 345 (1985).
17. H. Kaji, K. Nakanishi, N. Soga, and F. Horii, *J. Non-Cryst. Solids* **145**, 80 (1992).
18. J.C. Pouxviel, J.P. Boilot, J.C. Beloeil, and J.Y. Lallemand, *J. Non-Cryst. Solids* **89**, 345 (1987).
19. R.K. Iler, *The Chemistry of Silica* (Wiley, New York, 1979).
20. C.J. Brinker, *J. Non-Cryst. Solids* **100**, 30 (1988).
21. P.J. Flory, *Principles of Polymer Chemistry* (Cornell University Press, Ithaca, New York, 1971).
22. K. Nakanishi, H. Kaji, and N. Soga, in *Ceramic Transactions, Vol. 31, Porous Materials*, edited by K. Ishizaki et al. (American Ceramics Society, Ohio, 1993).
23. M. Takenaka, K. Tanaka, and T. Hashimoto in *Contemporary Topics in Polymer Science, Vol. 6, Multiphase Macromolecular Systems Symposium*, edited by W.M. Culberston (Plenum, New York, 1989).
24. T. Hashimoto, M. Takenaka, and T. Izumitani, *J. Chem. Phys.* **97**, 679 (1992).